Fall 2013

Using the piezoelectric backscatter signal for remote sensing of neural signals

Eren Alay
New Jersey Institute of Technology

Copyright Warning & Restrictions

The copyright law of the United States (Title 17, United States Code) governs the making of photocopies or other reproductions of copyrighted material.

Under certain conditions specified in the law, libraries and archives are authorized to furnish a photocopy or other reproduction. One of these specified conditions is that the photocopy or reproduction is not to be "used for any purpose other than private study, scholarship, or research." If a, user makes a request for, or later uses, a photocopy or reproduction for purposes in excess of "fair use" that user may be liable for copyright infringement,

This institution reserves the right to refuse to accept a copying order if, in its judgment, fulfillment of the order would involve violation of copyright law.

Please Note: The author retains the copyright while the New Jersey Institute of Technology reserves the right to distribute this thesis or dissertation

Printing note: If you do not wish to print this page, then select "Pages from: first page # to: last page #" on the print dialog screen

ABSTRACT

USING THE PIEZOELECTRIC BACKSCATTER SIGNAL FOR REMOTE SENSING OF NEURAL SIGNALS

by
Eren Alay

In recent studies, various methods to sense neural signals are used and new methods for remote sensing of neural signals are being developed. However, there are still major difficulties in building long-term implantable neural interface systems that can reliably record neural activity and serve as the basis of brain-machine interfaces (BMI). Therefore, this research is conducted to design a remote neural sensing system that is based on modulation of the backscatter signal from a piezoelectric element by the neural signals. The hypothesis is that if the neural signal is detected with a simple amplifier and the output of this amplifier is connected in parallel to a piezoelectric element, the backscattered signal from the piezoelectric element should be modulated by the neural signal amplitudes. To this end, the echo signal from the piezoelectric element is analyzed and the effect of a load resistor is demonstrated. And then, an electronic circuit to implement the modulation function is simulated on the computer and constructed. The experimental results support the main hypothesis of the project.

USING THE PIEZOELECTRIC BACKSCATTER SIGNAL FOR REMOTE SENSING OF NEURAL SIGNALS

by
Eren Alay

A Thesis
Submitted to the Faculty of
New Jersey Institute of Technology
in Partial Fulfillment of the Requirements for the Degree of
Master of Science in Biomedical Engineering

Department of Biomedical Engineering

January 2014

APPROVAL PAGE

USING THE PIEZOELECTRIC BACKSCATTER SIGNAL FOR REMOTE SENSING OF NEURAL SIGNALS

Eren Alay

Dr. Mesut Sahin, Thesis Advisor — Date
Associate Professor of Biomedical Engineering, NJIT

Dr. Raquel Perez-Castillejos, Committee Member — Date
Assistant Professor of Biomedical Engineering, NJIT

Dr. Max Roman, Committee Member — Date
Assistant Research Professor of Biomedical Engineering, NJIT

BIOGRAPHICAL SKETCH

Author: Eren Alay

Degree: Master of Science

Date: January 2014

Undergraduate and Graduate Education:

- Master of Science in Biomedical Engineering,
  New Jersey Institute of Technology, Newark, NJ, 2014

- Bachelor of Science in Electronics Engineering,
  Ankara University, Ankara, Turkey, 2011

Major: Biomedical Engineering

Publication:

Abhineet Mishra, Deniz Ozgulbas, Eren Alay, Eun H. Kim, Tara L. Alvarez, "Checking the saliency of the stimuli on central versus peripheral visual field", 39th Annual Northeast Bioengineering Conference (NEBEC'13), Syracuse, NY, April 2013.

To goodness of endeavoring

ACKNOWLEDGMENT

First and foremost, I would like to thank warmly Dr. Mesut Sahin, my thesis advisor, for his great guidance. He gave me the chance to work on his recently developed concept, and encouraged and challenged me throughout various stages of this thesis. Without his consistent and illuminating support, this thesis could not have reached its present form.I would also like to thank Dr. Raquel Perez-Castillejos and Dr. Max Roman for their valuable suggestions, remarks and insight.

Finally, due to their sincere attitude and approach without provision, I owe my special gratitude to all the members of Neural Interface Laboratory.

TABLE OF CONTENTS

TABLE OF CONTENTS
(Continued)

Chapter **Page**

TABLE OF CONTENTS
(Continued)

LIST OF TABLES

LIST OF FIGURES

LIST OF FIGURES

(Continued)

LIST OF FIGURES

(Continued)

CHAPTER 1

INTRODUCTION

1.1 Background

1.1.1 Ultrasound: As a Way of Recording

Several studies indicated that the ultrasound can produce significant impact on neural tissue. It has been used as a way of stimulation of receptors in the skin and soft tissue, peripheral nerves, the brain, cochlea and also used for pain management and treatment of spasticity (Colucci, Strichartz, Jolesz, Vykhodtseva, & Hynynen, 2009; Gavrilov, Tsirulnikov, & Davies, 1996). But, it has major challenges before it can become a way of a tetherless, high density, low power neural recording method. Currently, the recordings of neural activities from different regions of the nervous system are done via direct electrical connections using fine wires. Thus, ultrasonic approach could set the stage for a unique method of a wireless neural interface.

1.1.2 Remote Neural Signal Sensing

Use of implantable multi-electrode arrays (MEAs) has become popular in modern neuroscience research to investigate neural activity in the central nervous system. By observing the action potentials of many neurons in specific brain areas or in a localized region of the spinal cord, it is possible to obtain the functional information related to the motor, auditory, olfactory, and visual activities (Gosselin, 2011; Harrison, Jan 2007; Obeid, Nicolelis, & Wolf, 2004; Roy & Wang, 2012). Data is acquired through the implanted electrodes using wired connections. Thus, it is inevitable to face the risk of

infection, wire breakage, tissue damage, and, and interfering signals due to the high impedance electrodes in the context of low signal levels associated with neural signal (Ferguson & Redish, 2011; N. Neihart & Harrison, 2004; N. M. Neihart & Harrison, 2005). To alleviate these problems, wireless transmission and recording of the electrophysiological data should be developed. In addition, according to the recent theoretical study, an ultrasonic, low power solution for recording neural signals is feasible (Seo, Carmena, Rabaey, Alon, & Maharbiz, Jul 2013).

Although wireless radiofrequency telemetry systems are also being tested in recent studies, due to the low transmission efficiency through biological tissues and large power demands, new approaches are needed (Ferguson & Redish, 2011). Undoubtedly, several issues such as safety, insertion method, tissue response, and power should be taken into consideration in the development of implantable, wireless neuroprostheses (Ferguson & Redish, 2011).

1.2 Objective

The aim of this thesis is to investigate a remote neural activity sensing method that does not require large penetrating shank electrodes into the CNS parenchyma. The thesis proposes a novel method for sensing the neural signals using an implanted piezoelectric piece and transmitting the signals to an outside receiver using the backscattering of ultrasound waves generated externally. In this paradigm, each piezoelectric piece serves as a single channel of recording. To this end, the backscattered echo signal detected by external piezoelectric element was analyzed. The modulation of the backscatter signal by varying the load resistor of the implanted unit was investigated.

As a starting point, the type of piezoelectric material that would be most suitable for this study was evaluated, and lead zirconate titanate (PZT) was chosen for the circuitry. Resonance and anti-resonance frequencies of the material were measured. Furthermore, to observe the effect of the load resistor and backscatter signal modulation, a potentiometer (1000 Ω) was connected parallel to the PZT assembly. As the final step, the circuitry was designed in light of these preliminary measurements and a series of computer simulations.

The thesis is divided into six chapters. This chapter presents the objectives and background information including the review of related studies conducted by other researchers and explains the significance of the work performed. Chapter 2 and Chapter 3 review the theoretical background for this work. A brief view of the experimental set-up developed for load resistor effect measurements is given in Chapter 4 and Chapter 5 deals with simulation, practical results and discussion. Finally, Chapter 6 presents the summary of the work along with conclusions and future outlook.

CHAPTER 2

PERTINENT ASPECTS OF ULTRASONIC WAVE THEORY

2.1 Ultrasonic Wave Properties

Ultrasound can travel through the tissues of the body either longitudinally or transversely. In general, bone is the only medium in which transverse waves (shear waves) are important. For soft tissue and liquid, ultrasound waves propagate as longitudinal waves.

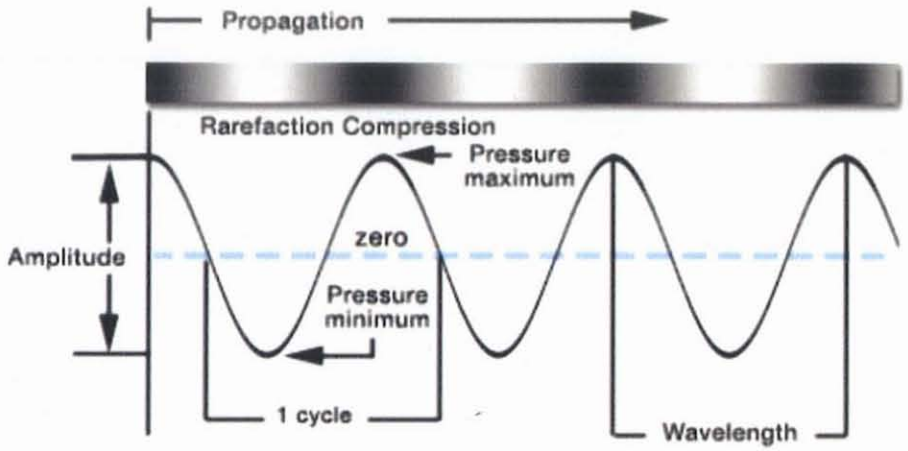

Figure 2.1 Where particles in adjacent regions have moved towards each other, a region of compression (increased pressure) results, but where particles have move apart a region of rarefaction (reduced pressure) results.
Source: (Hoskins, Jun 2010).

2.1.1 Frequency, Velocity and Wavelength

One cycle of an ultrasound wave comprises of a region of compression an adjacent region of rarefaction. The distance included by one cycle is the wavelength of the ultrasound wave. The number of cycles per unit time is referred to as the frequency of the wave. The relationship between frequency and wavelength is expressed using the equation:

$$\lambda = \frac{c}{f} \tag{2.1}$$

where λ is the wavelength of the ultrasound wave , f is the frequency, c is the speed of the wave. In ultrasound, the term propagation speed is preferred over the term velocity (Hendee, 2002).

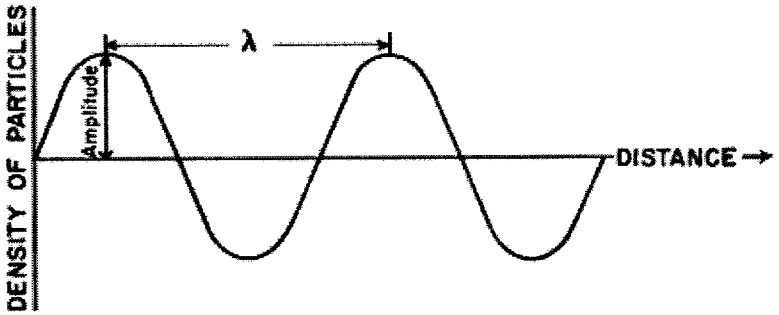

Figure 2.2 Characteristics of an ultrasound wave. A wave cycle can be represented as a graph of local pressure (particle density) in the medium versus distance in the direction of the ultrasound wave.
Source (Hendee, 2002).

The molecular velocity describes the velocity of the individual molecules in medium, whereas the wave velocity describes the velocity of the ultrasound wave through the medium (Hendee, 2002). Therefore, it can be stated that the velocity of ultrasound in a medium is virtually independent of the ultrasound frequency (Hendee, 2002). As another property, phase describes the position within a cycle of oscillation.

Table 2.1 Approximate Velocities of Ultrasound in Selected Materials

Nonbiologic Material	Velocity (m/s)	Biologic Material	Velocity (m/s)
Acetone	1174	Fat	1475
Air	331	Brain	1560
Aluminum (rolled)	6420	Mineral oil	1480
Ethanol	1207	Spleen	1570
Glass (Pyrex)	5640	Blood	1570
Mercury	1450	Muscle	1580
Nylon (6-6)	2620	Lens of eye	1620
Polyethylene	1950	Skull bone	3360
Water (distilled), 25°C	1498	Soft tissue (mean value)	1540

Source: (Hendee, 2002).

2.1.2 Intensity and Power

As the sound wave passes through the medium, it transmits energy from the source into the medium. The rate of energy transmission is referred as power. The ultrasound produced by the source travels through the tissues of body along an ultrasound beam, and the associated power is not distributed evenly across the beam, but might be more concentrated near the center (Hoskins, Jun 2010). The intensity is the measure of the amount of power flowing through an area of the beam cross section (Hoskins, Jun 2010). Intensity is usually defined relative to some reference intensity (Hendee, 2002). In acoustics, the decibel scale is used, with the decibel defined as:

$$\mathrm{dB} = \log\frac{I}{I_0} \tag{2.2}$$

where I_0 is the reference intensity. It may be also stated that ultrasound wave intensity is related to maximum pressure (P_m) in the medium by the following equation:

$$I = \frac{P_m{}^2}{2\rho c} \tag{2.3}$$

where ρ is the density of the medium in grams per cubic centimeter and c is the velocity of sound in the medium.

2.2 Possible Interactions of Ultrasonic Wave

When an ultrasound wave propagating through one type of medium, it encounters different medium and several occasions arise like scattering, reflection, refraction, absorption or transmission. Due to the acoustic impedance difference between types of tissues, the energy of the ultrasonic wave is reflected back towards the source of the wave, while the remainder is transmitted into the second tissue.

Acoustic impedance of a medium is a measure of the response of the particles of the medium in terms of their velocity (Hoskins, Jun 2010). Acoustic impedance is determined by either the equation relied on medium's density and stiffness or the equation depended on the parameters of both velocity of the sound in the medium and medium's density:

$$Z = \rho c \tag{2.4}$$

Table 2.2 Acoustic Impedance of Selected Materials

Material	**Z, MRayls**	**Material**	**Z, MRayls**
PZT(ceramic)	30	Muscle	1.70
PVDF	2.7	Blood	1.67
Air	0.0004	Brain	1.60
Water	1.54	Bone	6.47

2.2.1 Attenuation

During the travel of the ultrasound beam, several processes demonstrated in Figure 2.3 can arise. Briefly, attenuation is a term used to account for loss of wave amplitude due to all mechanisms (Hendee, 2002). This loss is defined as the ratio of two amplitudes:

$$L[dB] = 20 \log \frac{A_{in}}{A_{out}} \tag{2.5}$$

where A_{out} and A_{in} denote the amplitude with and without attenuation, respectively.

Contributions to attenuation of an ultrasound beam may include absorption, reflection, refraction, scattering, diffraction, interference, divergence (Hendee, 2002).

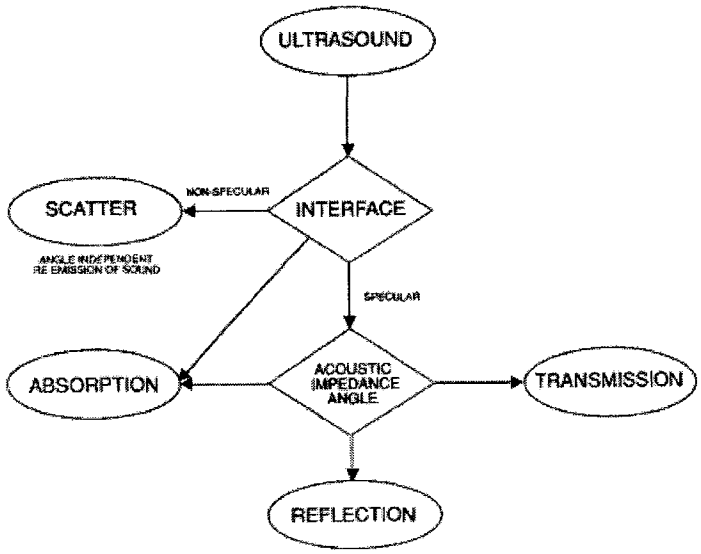

Figure 2.3 Summary of interactions of ultrasound at boundaries of materials.
Source: (Hendee, 2002).

The attenuation of the medium leads to loss which is proportional to the propagation distance, i.e., the total loss can be expressed as:

$$L = \alpha d f \tag{2.6}$$

where d is the propagation distance, f is the frequency of incident ultrasound beam and α is the so-called attenuation coefficient. Attenuation coefficient of different media shows complex patterns as a function of frequency.

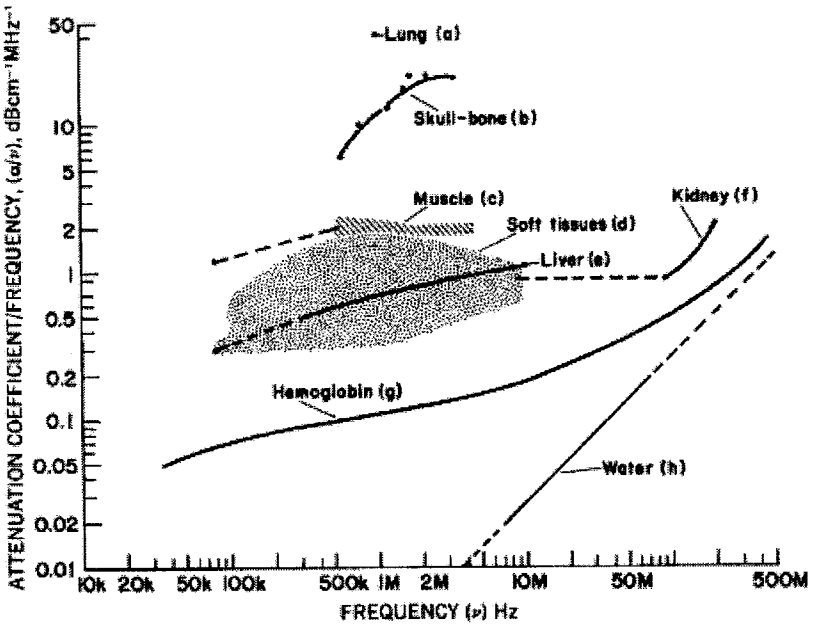

Figure 2.4 Ultrasound attenuation coefficient as a function of frequency for various tissue samples.
Source: (Hendee, 2002).

The attenuation of ultrasound in a material is defined by attenuation coefficient α in units of decibels per centimeter and it is the sum of the individual coefficient for scattering and absorption.

$$\alpha = \alpha_{absorption} + \alpha_{scattering} \tag{2.7}$$

Severe attenuation usually occurs only at high frequencies while at low frequencies beam spread is the predominant cause of loss over large propagation distances.

Table 2.3 Attenuation Coefficients for 1 MHz Ultrasound

Material	α(dB/cm)	Material	α(dB/cm)
Blood	0.18	Lung	40
Fat	0.6	Liver	0.9
Muscle (across fibers)	3.3	Brain	0.85
Muscle (along fibers)	1.2	Kidney	1.0
Aqueous and vitreous humor of eye	0.1	Spinal cord	1.0
Lens of eye	2.0	Water	0.0022
Skull bone	20	Caster oil	0.95

Source: (Hendee, 2002).

As it is shown in Table 2.3, in bone tissue, attenuation of ultrasound is high whereas little attenuation appears in water because of the fact that attenuation coefficients are very large and small respectively in each medium.

2.2.2 Absorption

Ultrasound is "absorbed" by the medium if part of the beam's energy is converted into other forms of energy, such as an increase in the random motion of molecules. Absorption is the main form of attenuation. . It happens that as sound travels through soft tissue, the particles that transmit the waves vibrate, cause friction, a loss of sound energy occurs and heat is produced. Absorption is likely to be stronger at frequencies which excite natural modes of vibration of the particular molecules of the medium as it is at such frequencies that they are most out of step with the passing wave (Hoskins, Jun 2010).

As it is seen in Equation (2.7), there is a complementary relationship between the individual coefficients of scattering and absorption. While scattering accounts for the larger part of attenuation in some materials such as polycrystalline metals and ceramics, absorption is the dominant loss in others such as polymers and fluids (Nagy). For

example, in water, which is often used as a coupling medium, the absorption coefficient can be expressed:

$$\alpha_{water}[dB/m] \approx 0.2f^2[MHz] \tag{2.8}$$

where f denotes frequency.

2.2.3 Scattering

Scattering can be described as the event that refers to the change with a less orderly fashion in the ultrasound beam direction. The behavior of a sound beam when it encounters an obstacle depends upon the size of the obstacle compared with the wavelength of the sound (Hendee, 2002). If the size of the obstacle is smaller than the wavelength of the ultrasound, the obstacle will scatter energy uniformly in various directions whereas for targets of the order of a wavelength in size, scattering will not be uniform in all directions but will still over a wide range (Hendee, 2002; Hoskins, Jun 2010). Some of the ultrasound energy may return to its original source after non-specular scatter, but probably not until many scatter events have occurred (Hendee, 2002).

The total ultrasound power scattered by a very small target is much less than that for a large interface and is related to the size d of the target and the wavelength λ of the wave. For the situation in which the targets are much smaller than a wavelength ($d \ll \lambda$), scattered power can be expressed:

$$W_{scattered\ power} \propto \frac{d^6}{\lambda^4} \propto d^6 f^4 \tag{2.9}$$

where f is the frequency of the wave. And this scattering process is referred to as Rayleigh scattering (Hendee, 2002; Hoskins, Jun 2010).

2.2.4 Reflection

When an ultrasound wave propagating through one medium meets an interface with a second medium of different acoustic impedance, some of the wave is transmitted into the second medium and some is reflected back to the first one.

For an ultrasound wave incident perpendicularly upon an interface, the fraction α_R of the incident energy that is reflected (i.e., the reflection coefficient α_R) is:

$$\alpha_R = \left(\frac{Z_2 - Z_1}{Z_2 + Z_1}\right)^2 \tag{2.10}$$

where Z_1 and Z_2 are the acoustic impedances of the two media. The fraction of the incident energy that is transmitted across an interface is described by the transmission coefficient α_T, where

$$\alpha_T = \frac{4Z_2Z_1}{(Z_2 + Z_1)^2} \tag{2.11}$$

And it should be stated that

$$\alpha_R + \alpha_T = 1 \tag{2.12}$$

This is the basis of ultrasound as different organs in the body have different densities and acoustic impedance and this creates different degrees of reflections. In some cases the acoustic impedance can be so great that all the sound wave energy can be reflected. This happens when sound comes in contact with bone and air. This is the reason why ultrasound is not used as a primary imaging modality for bone, digestive tract and lungs.

2.2.5 Refraction

When an ultrasound beam obliquely crosses an interface between two different media, its direction will be changed. If the velocity of ultrasound is higher in the second medium,

then the beam enters this medium at a more oblique (larger angle with the normal) angle. This behavior of ultrasound transmitted obliquely across an interface is termed as refraction (Hendee, 2002). The relationship between incident and refraction angles is described by Snell's law:

$$\frac{\sin \theta_i}{\sin \theta_r} = \frac{c_i}{c_r} \tag{2.13}$$

where θ_i and θ_r are the incidence and refractive angle also c_i and c_r denote velocity in incidence medium and velocity in refractive medium, respectively.

CHAPTER 3

GENERATION AND DETECTION OF ULTRASONIC WAVES

3.1 Piezoelectric Materials and Their Basic Properties

3.1.1 Piezoelectricity and Piezoelectric Effects

All dielectric materials when subjected to an external electric field by the effect of the displacement of positive and negative charges within the material undergo change in dimensions (Vijaya, 2013).

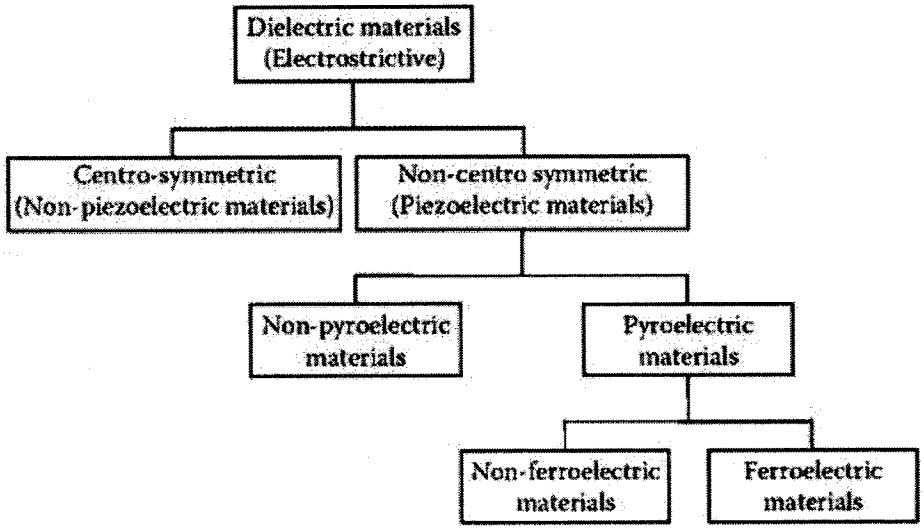

Figure 3.1 The dielectric materials can be classified in terms of their response to external stimuli.
Source: (Vijaya, 2013).

Different material characteristics are classified in a hierarchy as it is shown in Figure 3.1. Fundamentally, piezoelectric materials behave electrically polarized when the stress is introduced on it. And they can convert the mechanical energy to electrical energy

vice versa. On the other hand, pyroelectric materials are spontaneously polarizable and they are sensible to temperature. If the material spontaneously polarized and can remain like this with the absence of the electric field, they are called specifically as ferroelectric materials.

Piezoelectricity (electricity by pressure) was proposed by Hankel in 1881 to the name the phenomenon discovered a year before by the Pierre and Jacques Curie brothers who observed that positive and negative charges appeared on several parts of the crystal surfaces when comprising the crystal in different directions (Arnau, 2004; Safari, 2008).

The piezoelectric effect refers to the voltage produced between surfaces of a solid dielectric when a mechanical stress is applied to it. This process is specifically called direct piezoelectric effect (Vijaya, 2013).

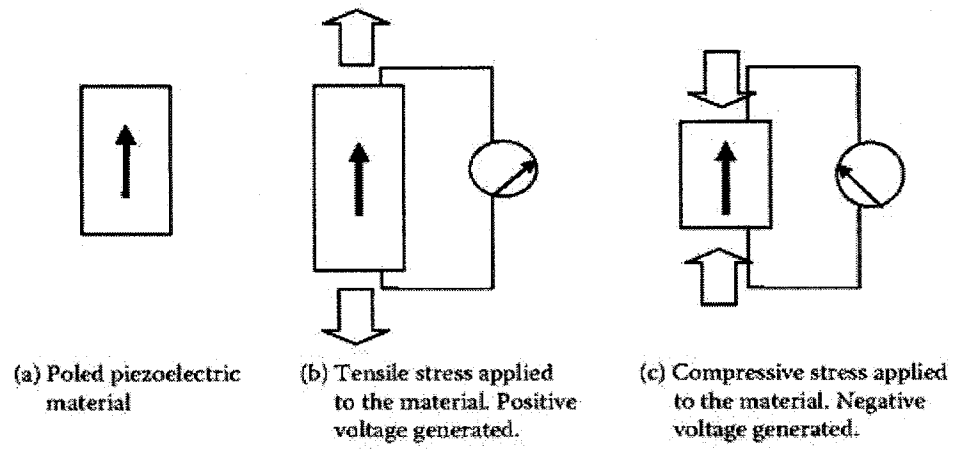

Figure 3.2 Direct piezoelectric effect: (a) Poled piezoelectric material. (b) When tensile stress is applied to the material, the material develops voltage across its face with the same polarity as the poling voltage. (c) When a compressive stress is applied to the material, the material develops voltage with polarity opposite to that of the poling voltage.
Source: (Vijaya, 2013).

Conversely, when a voltage is applied across certain surfaces of a solid which exhibits the piezoelectric effect, the solid undergoes a mechanical distortion. This is defined as indirect piezoelectric effect (Vijaya, 2013).

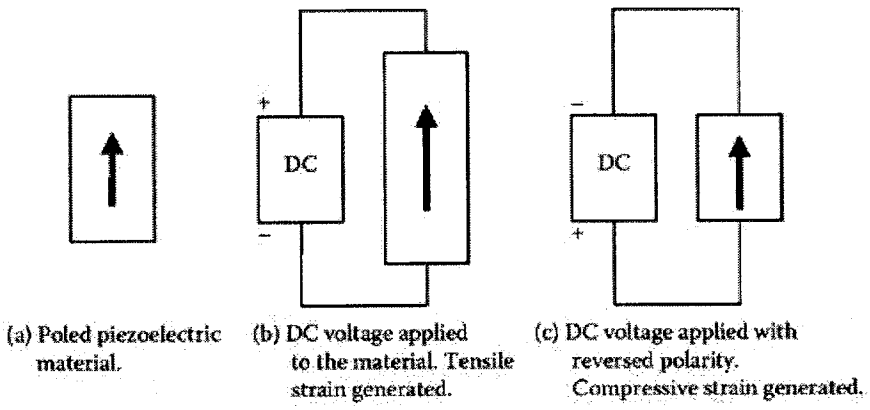

Figure 3.3 Indirect piezoelectric effect: (a) Poled piezoelectric material. (b) When a DC field is applied with the same polarity as the poling field, the material develops a tensile strain. (c) When a DC field is applied in the reverse direction, the material develops compressive strain.
Source: (Vijaya, 2013).

The alternating field makes the material to extend and contract alternately at the same frequency as the applied field. The vibration produces an ultrasonic field in the vicinity of the material. This effect is used for the generation of acoustic field (Vijaya, 2013).

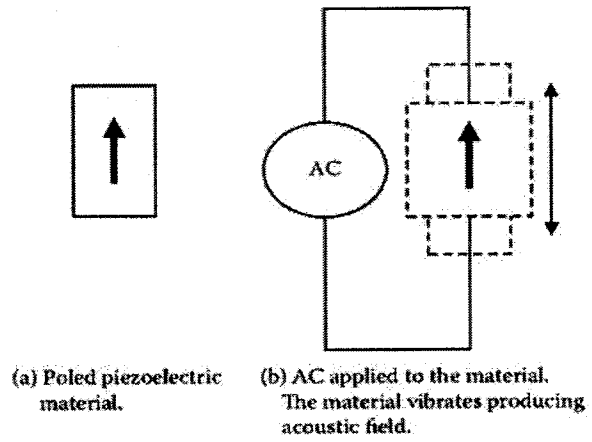

Figure 3.4 Effect of AC field on a piezoelectric material: (a) Poled piezoelectric material. (b) AC field is applied to the material.
Source: (Vijaya, 2013).

The direct and indirect piezoelectric effects have several applications such as generation and detection ultrasonic waves, pressure sensors, and actuators because of the fact that they have the ability to convert mechanical energy to electrical energy (direct piezoelectric effect) and electrical energy to mechanical energy (indirect piezoelectric effect).

3.1.2 Material Properties

As it is stated in the previous section, there are two forms of piezoelectric effect. In terms of the direct piezoelectric effect, the input is mechanical energy such as stress or strain and output refers the electrical energy that can be form of surface charge density, electric field or voltage. On the other hand, for the indirect piezoelectric effect, input denotes the electrical energy while output is mechanical energy. From this point, a brief description of some of relevant properties is stated below to understand the parameters those have an impact on behavior of a piezoelectric material or input and output parameters.

Piezoelectric coefficients, elastic constants and permittivity relate tensors and vectors. Hence, they each have matrix notations and they can be expressed with right-handed Cartesian coordinate system. That means in each direction, both input and output are represented. Due to the components of the tensors are all not independent, they can get reduced.

The stress produced in a piezoelectric material by the help of the electric field is called the piezoelectric constant e which has a unit of N/V m (Vijaya, 2013). The larger the magnitude of the stress constant leads to the greater the coupling between elastic and electrical effects. As another coefficient, piezoelectric strain constant d is the produced strain while applying the electrical field with no external stress and it can be called as a transmitting constant with the unit of m/V (Vijaya, 2013). The electrical field produced per unit of applied stress is known as the receiving constant g, with the unit of V m/N (Vijaya, 2013). The dielectric parameter of interest in piezoelectric materials is the permittivity ε, which relates the vectors of the coefficients d and e (Vijaya, 2013). It determines the electrical impedance of the piezoelectric material. A large dielectric constant affects enabling a good electrical impedance match to the system electronics (Devaraju, 2013). The relationship between the d and e coefficients is defined as (Vijaya, 2013)

$$d = \varepsilon e \tag{3.1}$$

If the dielectric permittivity of a piezoelectric material is low, then the input electrical impedance will be high, that means higher drive voltage to generate the required acoustic output power (Devaraju, 2013). Furthermore, another parameter is the piezoelectric coupling coefficient k which reflects the efficiency of a piezoelectric

material as a transducer (Vijaya, 2013). It quantifies the ability of the piezoelectric material to convert the mechanical energy into electrical and vice versa. If loss of energy occurs during the conversion process, it will cause both loss of sensitivity and bandwidth (Devaraju, 2013). It is defined by Equation (3.2) (Vijaya, 2013).

$$k^2 = \frac{(piezoelectric\ energy\ density\ stored\ in\ the\ material)^2}{electrical\ energy\ density \times mechanical\ energy\ density} \tag{3.2}$$

It also can be obtained in terms of piezoelectric constants. The coupling coefficient is the ratio of usable energy delivered by the piezoelectric element to the total energy taken up by the element itself (Vijaya, 2013). The larger the value of k leads to the higher the piezoelectric coupling between the acoustic and electrical properties of the material. It is one of the important factors to get higher acoustic output power by means of dielectric constant relation. Higher acoustic output power gives the better measure of the acoustic radiating power of the transducer (Devaraju, 2013). Theoretically, manufacturers regularly determine the k values in the range of 30%-75% and practically, k values depend on the design of the device and the directions of the applied stimulus and the measured response (Vijaya, 2013). In addition to these properties, dissipation factors, electrical and mechanical loss tangent, are also taken into account. The larger mechanical loss decreases the response time resulting in improvement in the sharpness of the response, although it reduces the response amplitude considerably (Devaraju, 2013). Moreover, the mechanical quality factor Q_m is the reciprocal of the mechanical loss tangent whereas the electrical quality factor is the reciprocal of the electrical loss tangent. With increase in electrical loss tangent, conversion loss will increase due to dissipation of energy within the transducer. The dielectric loss will not affect the response time but the amplitude will be decreased slightly (Devaraju, 2013).

3.1.3 Dynamic Behavior of a Piezoelectric Material

For the analysis of dynamic behavior of a vibrating piezoelectric material, either mechanical or electrical equivalent systems can be used. In this case, to focus on the electrical representation would be more meaningful (Figure 3.5).

The vibrating force applied to the material is analogous to an alternating voltage. The piezoelectric element behaves as a capacitor of capacitance C_0

$$C_0 = \frac{\varepsilon A}{d} \tag{3.3}$$

where ε is the permittivity of the material and A and d are the area and thickness of the element, respectively. Inductance L is equivalent to the mass of the piezoelectric element and compliance constant is equivalent to the capacitor C. Furthermore, the energy loss because of the friction is equivalent to the energy loss because of the electrical resistance r in the circuit.

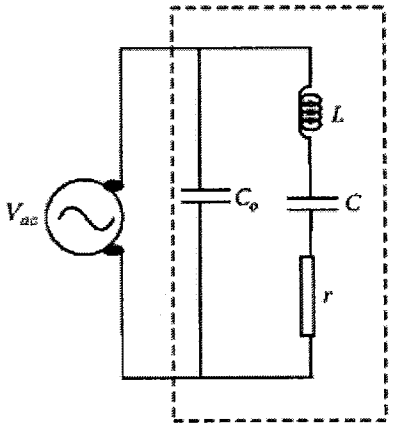

Figure 3.5 Equivalent electrical circuit representation of vibrating piezoelectric element. Source: (Vijaya, 2013).

The impedance of vibrating system is a function of frequency. The impedance has a minimum and a maximum. When the impedance is a minimum, the frequency for this

situation is called resonance frequency and for the maximum impedance, the frequency is called antiresonance frequency.

At the resonance frequency f_r the piezoelectric system's output reaches maximum amplitude. The resonance frequency f_r is equal to the series resonance frequency f_s at which the impedance of the equivalent circuit is zero, assuming that the resistance in the absence of the mechanical loss is zero:

$$f_r = f_s = \frac{1}{2\pi}\sqrt{\frac{1}{LC}} \tag{3.4}$$

The antiresonance frequency f_a approximates to the parallel resonance frequency f_p of the equivalent circuit, assuming that the resistance in the absence of the mechanical loss is zero:

$$f_a = f_p = \frac{1}{2\pi}\sqrt{\frac{C+C_0}{LCC_0}} \tag{3.5}$$

By the help of f_r and f_a, electromechanical coupling coefficient k can be evaluated (San Emeterio, 1997; Vijaya, 2013).

3.2 Piezoelectric Materials

Several piezoelectric materials according to their features are used in various applications such as detection of mechanical vibrations, fabrication of micro-electrical-mechanical-systems (MEMS) generation of ultrasonic and acoustic vibration and ultrasonic medical imaging.

3.2.1 Quartz

The most common material utilizes the piezoelectric effect of a certain crystalline material such as quartz which is a non-ferroelectric, natural occurring material. Due to

the piezoelectric effect profile of the quartz, it can be used in a feedback system to get an extremely stable frequency control (Vijaya, 2013). It has some unique sides that make it advantageous over other materials such as robust mechanical properties, high stiffness constant, high Q factor, good reliability, and long life (Vijaya, 2013).

3.2.2 Piezoceramic

Many piezoelectric materials besides quartz are available like lead zirconate titanate (PZT) which is a kind of ceramics. PZT is a ferroelectric ceramic that is commonly used in most of the transducer and actuator applications. The reason to be highly preferred is its good electromechanical coupling coefficient in thickness mode (k = 0.50), high relative dielectric constant (600), and low mechanical loss ($\tan\delta_m = 0.004$), and dielectric loss ($\tan\delta_e = 0.002$) (Devaraju, 2013). But the fact that it is fragile, low reproducibility, and fabrication difficulties are listed as its disadvantages.

Because of the high acoustic impedance of piezoceramic (34 MRayls) compared to human tissue (1.7 MRayls), there is an acoustic mismatch (Devaraju, 2013). Owing to this mismatch, great amount of reflection of acoustic waves at the interface causes a very sharp resonant peak, resulting in narrow bandwidth. It also leads to an impulse response ringing for several cycles, and inefficient power transfer. To overcome these problems, between the ceramic and tissue matching layers that have intermediate impedances are required (Schwartz, 2003). Because of PZT's recognized limitations such as high acoustic impedance and brittle nature, above 15 MHz it is usually not the material of choice (Foster, Harasiewicz, & Sherar, 2000; Zhang, 2008).

3.2.3 Piezopolymer

According to the research of Kawai in 1969, the discovery of a large remnant polarization in oriented films of PVDF was stated (Brown, 2000). It is the best known and most commercially active example of semicrystalline polymer and its dielectric and piezoelectric properties of PVDF depend on temperature except electromechanical coupling coefficient. Specifically, center frequency and bandwidth vary with temperature while the acoustic velocity of PVDF decreases. Therefore, the acoustic impedance and the resonance frequency of the PVDF-made-transducer decrease similarly with temperature.

Due to its highly flexible constitution, low acoustic impedance and other superior mechanical properties, PVDF becomes a new opportunity to design and develop more efficient transducers in high frequency ranges. Because the acoustic impedance of PVDF (4 MRayls) is close to that of water (1.5 MRayl) and muscle (1.7 MRayl), the reflection at the interface between transducer and the medium of propagation is minimized. Hence there is no need for matching layers which limits the bandwidth generally. Early polymer transducers demonstrating spectacular bandwidths of over 100% were routinely achieved (Foster et al., 2000). However, the comparatively low coupling efficiencies of 0.15 to 0.20 of the polymer material compromised performance in the diagnostic frequency range (Foster et al., 2000). By far, the optimum frequencies for successful applications of piezopolymer materials have stated at frequencies above 15 MHz (Foster et al., 2000). According to the research, it was shown that planar PVDF transducers can produce plane wave performance in the acoustic near field, which makes piezopolymer materials better than piezoceramics (Foster et al., 2000).

On the other hand, its low thickness mode electromechanical coupling factor (k = 0.20), which governs the transmitting efficiency, causes less acoustic output generation compared to PZT. Larger k contributes to the increase in the response amplitude. It has large dielectric loss factor ($\tan\delta_e$ = 0.25), which will lead to electric power being dissipated in the transducer itself (Foster et al., 2000). It has low relative dielectric constant, which will result in very high input electrical impedance in comparison to that of a PZT (Foster et al., 2000). Therefore, to generate equal amount of output acoustic power, a higher drive voltage is required for PVDF transducer. The capacitance of the transducer is proportional to the dielectric constant, which implies that the voltage developed across the transducer in the receiving mode is inversely proportional to its dielectric constant (Foster et al., 2000). Low dielectric constant is advantageous in terms of developing large voltage signal.

3.2.4 Piezocomposite

Piezocomposite materials are made of the combination of piezoelectric ceramic and ferroelectric polymer. In recent research, they are getting more popular since they exhibit high piezoelectric and pyroelectric properties, low acoustic impedance matching with water, and the feature of easy to be tailored to various requirements (Zhang, 2008). Their electro-acoustic efficiency can be improved with electromechanical coupling coefficient and they generate a short pulse with increase in amplitude compared to PZT resulting in increased bandwidth (Devaraju, 2013; Zhang, 2008). As a result, ceramic-polymer composites are the promising materials for applications in high-pressure sensors, hydrophones and shock accelerometers (Zhang, 2008).

3.3 Vibration Modes of Piezoelectric Materials

As it is mentioned at the beginning of the Chapter 3, vibration of the materials exhibits acoustic energy. The mode of vibration is related to the geometry of the piezoelectric material (Devaraju, 2013). In a regular way, the vibration is required in one direction only but if there is some in other directions, that will cause artifacts and energy loss (Devaraju, 2013).

Usually, there are three modes of vibration: plate, thickness and bar mode. According to the plate mode, the width and the length are much larger than the thickness of the material. For the thickness mode, the length (l) is much larger than the width (w) and thickness (t). To reach the optimum efficiency in the thickness mode, the ratio of width (w) and thickness (t) should be smaller than 0.7 (Devaraju, 2013). In the bar mode, the thickness (t) is much larger than the length (l) and width (w). The acoustic velocity varies in different modes of vibration. To get effective performance, only one mode of the vibration should be aimed by selecting optimum relationship between length, width and thickness. Otherwise, obtaining poor performance can be an inevitable result.

3.4 Ultrasonic Transducers

The piezoelectric material is the functional component of an ultrasonic device which is called as ultrasonic transducer. The main components of the ultrasonic transducer are the active element, backing, and wear plate.

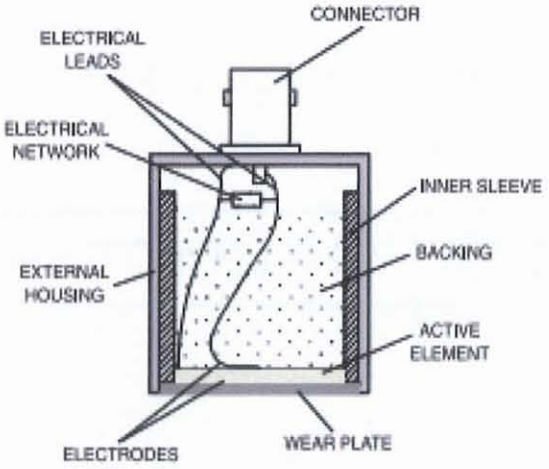

Figure 3.6 Typical ultrasonic transducer.
Source: Olympus NDT, 2006.

To drive the active element effectively, its thickness should equal to half of the wavelength, so that a compression wave reaches the opposite face of the material just as expansion is beginning to occur (Hendee, 2002). Despite the fact that a similar result is obtained for any odd multiple of half wavelengths (e.g., $3\lambda/2$, $5\lambda/2$), because of the additional attenuation effect, that is not reliable (Hendee, 2002). The resonance frequency of a material of half-wavelength thickness is calculated from Equation (2.1) where $\lambda=2l$. Another important point for the efficiency is acoustic impedance of the coupling medium. Transmission with minimum energy loss occurs when the impedance of the coupling medium is intermediate between the impedances of the piezoelectric material and the medium. The ideal impedance of the coupling medium is:

$$Z_{coupling\ medium} = \sqrt{Z_{transducer} \times Z_{medium}} \tag{3.6}$$

3.4.1 The Active Element

The active element, which is piezoelectric or ferroelectric material, converts electrical energy into ultrasonic energy. Materials used as active element are explained briefly in Subsection 1.5.4.

3.4.2 Backing

The backing is usually a highly damper, high density material that is used to control the vibration of the transducer by absorbing the energy radiating from the back face of the active element. When the acoustic impedance of the backing matches the acoustic impedance of the active element, the result will be a heavily damped transducer that displays good range resolution but may be lower in signal amplitude. If there is a mismatch in acoustic impedance between the element and the backing, more sound energy will be reflected forward into the test medium. Therefore, there is a trade-off between resolution and signal amplitude. If the low resolution is preferred, this may lead to high signal amplitude or great sensitivity.

3.4.3 Wear Plate

Mainly, the wear plate is used for protecting the transducer element from the testing medium. For some different purpose transducers, this component can be served to function as an acoustic transformer high acoustic impedance of the active element and the water.

3.5 Basic Parameters of Ultrasonic Transducer

3.5.1 Sound Field

The sound field of a transducer is divided into two zones; the near field and the far field. The near field is the region directly in front of the transducer where the echo amplitude goes through a series of maxima and minima and ends at the last maximum, at distance N from the transducer.

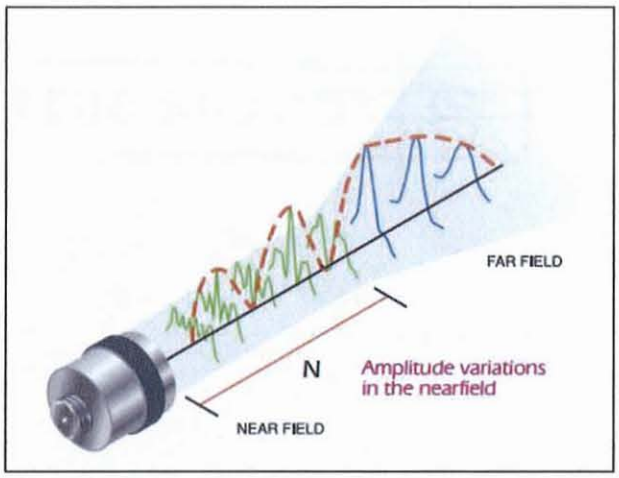

Figure 3.7 Demonstration of the near and far field of the transducer.
Source: Olympus NDT, 2006.

The near field distance can be calculated by the help of transducer frequency, element diameter, and the sound velocity of the test material as shown by Equation (3.7).

$$N = \frac{D^2 f}{4c} \tag{3.7}$$

where N denotes the near field, D is the element diameter, f is the frequency of the transducer and c is the material sound velocity.

3.5.2 Beam Diameter

The smaller the beam diameter, the greater the amount of energy is reflected by a testing material. The -6 dB pulse-echo beam diameter at the focus can be calculated with Equation (3.8).

$$BD[-6dB] = \frac{1.02Fc}{fD} \tag{3.8}$$

where BD denotes the beam diameter, F is the focal length, c refers to material sound velocity, f is the frequency of the transducer and D is the element diameter.

3.5.3 Focal Zone

The starting and ending points of the focal zone are located where the on-axis pulse-echo signal amplitude drops to - 6 dB of the amplitude at the focal point. The length of the focal zone is given by Equation (3.9):

$$F_z = N\left(\frac{F}{N}\right)^2\left[\frac{2}{\left(1+0.5\frac{F}{N}\right)}\right] \tag{3.9}$$

where F_Z denotes the focal zone, N is the near field and F refers to focal length.

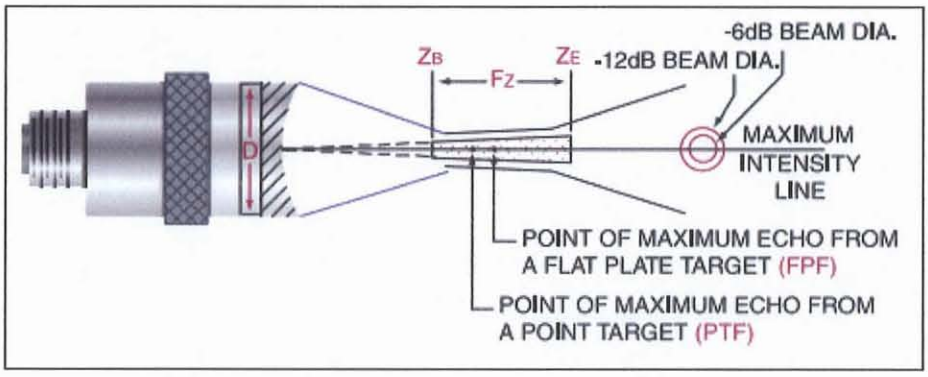

Figure 3.8 Other parameters of a sound beam. Z_B refers to beginning of the focal zone while Z_E is the ending of the focal zone.
Source: Olympus NDT, 2006.

CHAPTER 4

DESCRIPTION OF EXPERIMENTAL SYSTEM SET UP

4.1 Overall System Description

The system's main component is the piezoelectric material, PZT. In order to make acoustic signal measurements the experimental configuration is set up as shown in Figure 4.1.

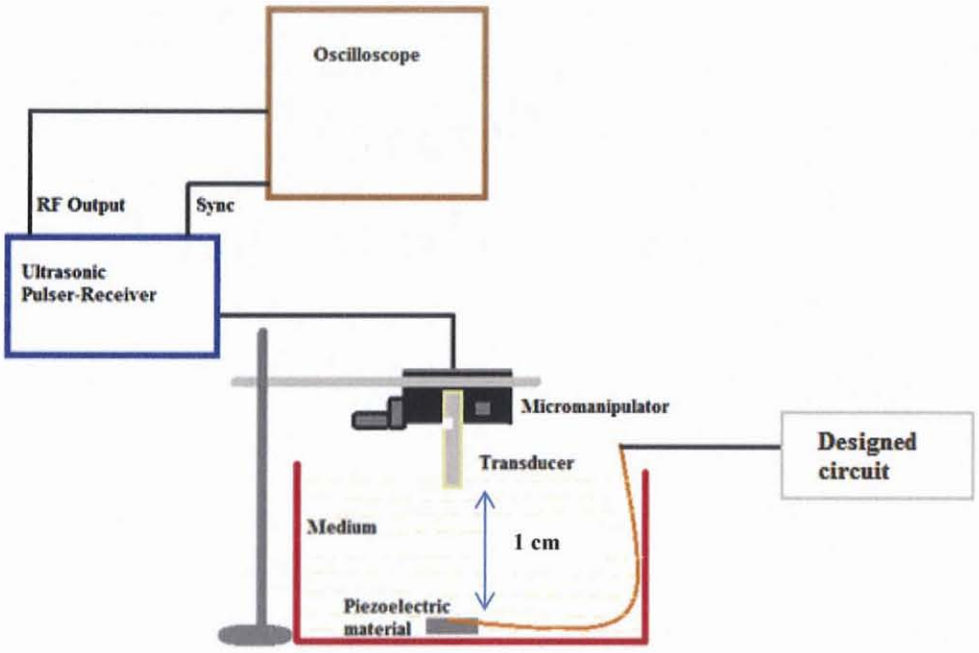

Figure 4.1 Experimental set up for acoustic measurements.

The transducer was mounted on a micromanipulator so that it was able to move the transducer in three orthogonal axes. The transducer was used in a transmitter-receiver mode. The piezoelectric material was glued on a metal piece for stabilization in the dish and kept at a distance of 1 cm from the transducer. The distance between the transducer and face of the piezoelectric material was determined according to the near field distance

and point target focus parameters of the transducer. Thus, 1 cm separation distance was chosen to evaluate the performance of the transducer effectively. To test the feasibility, modulated ultrasonic pulses reflected from the piezoelectric material was captured through the transmitter-receiver device, which has its own amplification and basic signal conditioning circuitry. The output of the transducer was displayed on the oscilloscope.

4.2 Ultrasound Pulser/Receiver

The ultrasonic square wave pulser/receiver model 5077PR (Olympus), shown in Figure 4.2, is a broadband ultrasonic pulser/receiver unit with a variable receiver gain.

Figure 4.2 The ultrasonic square wave pulser/receiver (Olympus 5077PR).

The pulser section of the instrument generates short, large-amplitude electric pulses. When these pulses applied to an ultrasonic transducer, they are converted into short acoustic pulses. These ultrasonic pulses are received either by the transmitting transducer (pulse-echo method), or by a separate receiving transducer (through-transmission method).

4.3 Ultrasonic Transducer

In this research, centrascan composite focused immersion transducer, which has 3.5 MHz center frequency and 6.35 mm element diameter, was chosen. The focal length of the transducer was 9.9 mm. The calculated near field distance using Equation (3.7) was obtained as 23.22 mm. By considering these specifications, the transducer was placed in the medium with optimum distance from the piezoelectric material.

Figure 4.3 Different cases of immersion transducer.

4.4 Piezoelectric Material

In this thesis, the sample of PZT (Piezo Systems Inc.) with 500 μm thickness was cut in dimension of 0.5 mm×0.5 mm. To make wire connections to the material, 0.11 mm thick insulated stainless steel wires were used. Because of the high temperature sensitivity of PZT, instead of soldering, the all-purpose grade, very fast setting epoxy adhesive (Epoxy Technology) was preferred for connection.

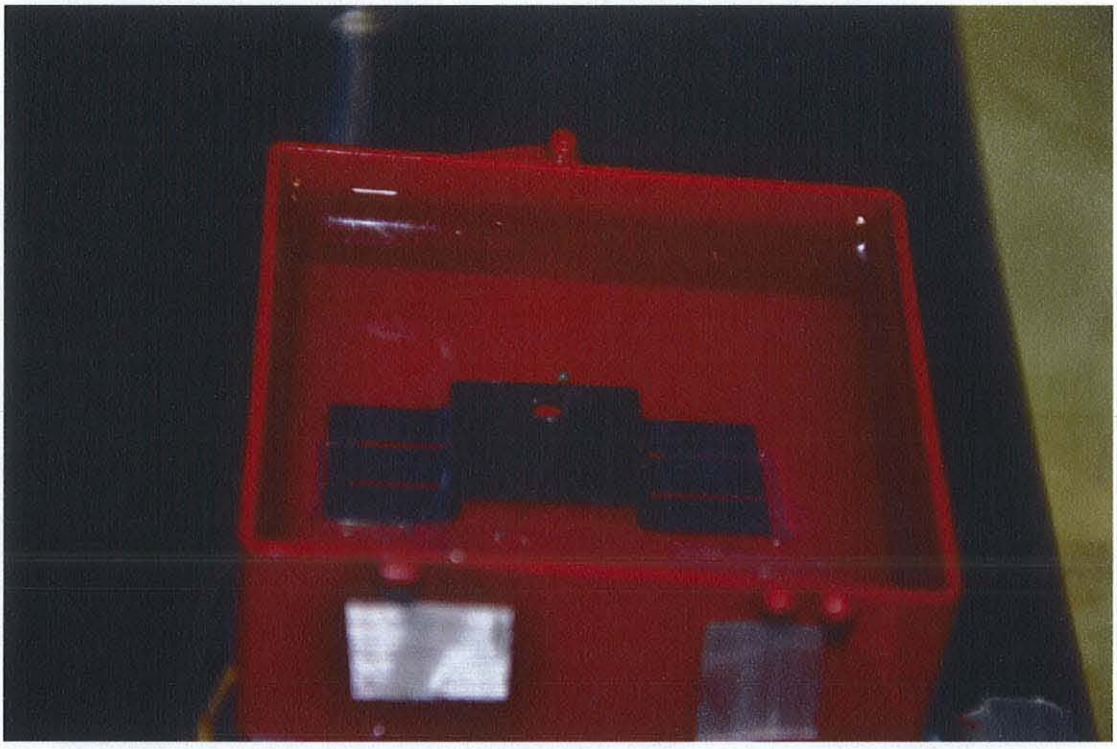

Figure 4.4 Prepared PZT sample attached to a heat sink for mechanical stability.

4.5 Other System Components

In addition, 15 MHz function/arbitrary waveform generator (Agilent 33120A) was used to generate the square wave pulses with regulated voltage amplitude for the implanted circuitry that would modulate the backscattered signals. The amplified output signal from the pulser/receiver was sent to oscilloscope (100 MHz, 400 MS/sec, Gould DSO 4074). A synchronizing pulse is also provided by pulser/receiver and was connected to the trigger input of the oscilloscope. The synchronizing pulse is necessary for obtaining steady view of the received signal.

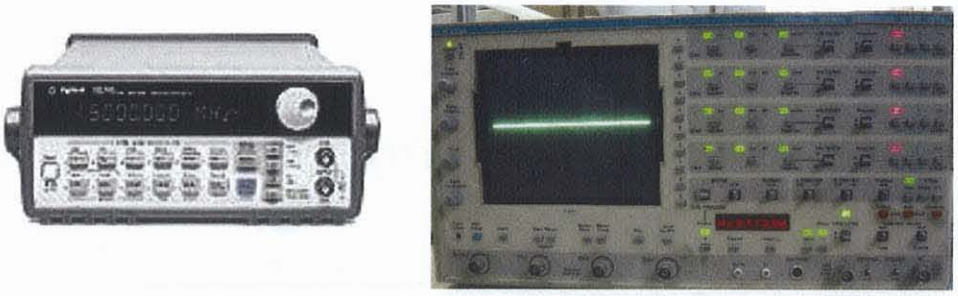

Figure 4.5 Agilent 33120A function/arbitrary waveform generator and Gould DSO 4074 oscilloscope.

CHAPTER 5

BACKSCATTER SIGNAL EVALUATION PROCESSES

5.1 Determining and Testing the Resonance Frequency of PZT

After the preparation of the piezoelectric assembly, electrical impedance of the piezoelectric material was measured as a function of frequency. In principle, the circuit relied on basic voltage divider concept (Figure 5.1). Then, the output voltage of the circuit shown in Figure 5.1 was plotted as a function of frequency to determine the resonance and anti-resonance frequencies for the PZT material with the given dimensions.

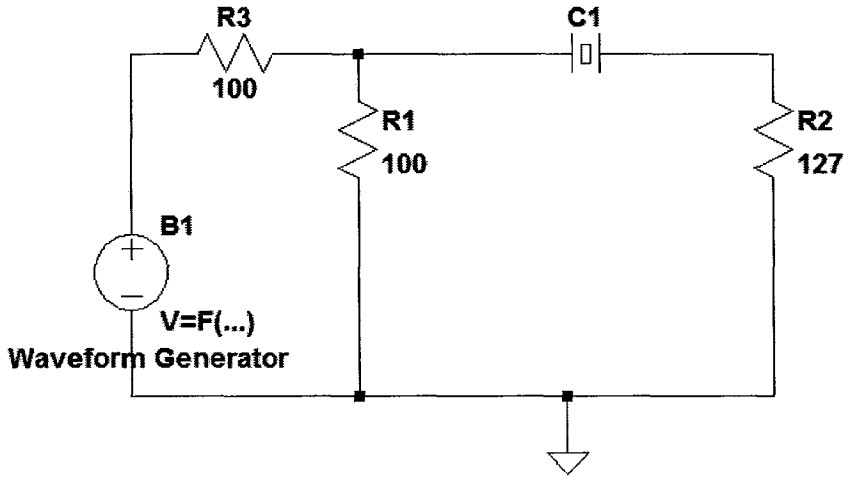

Figure 5.1 Circuit schematic for determining minimum impedance (resonance frequency) and maximum impedance (antiresonance frequency) of the piezoelectric element.

At the resonance frequency, the output (through R_2) voltage amplitude is at a maximum, because the piezoelectric impedance reaches its minimum. Therefore, the frequency when the output reaches a maximum is the resonance frequency, f_r, for the

piezoelectric piece, and the frequency when the output reaches its minimum is the antiresonance frequency, f_a.

5.1.1 Results and Discussion

By applying 5 V_{pp} sinusoidal wave varying from 50 kHz to 15 MHz, resonance and anti-resonance frequencies were obtained. According to the measurement results, two resonance frequencies were observed but specifically, in this work the resonance frequency that we are interested in is the second one (thickness mode), which was obtained at 4.1 MHz.

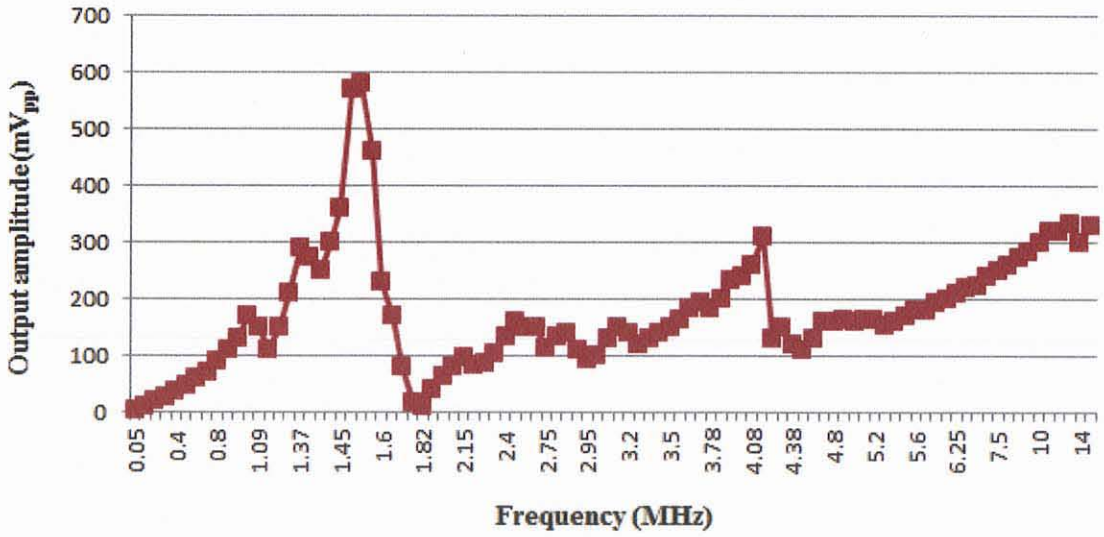

Figure 5.2 Determining the resonance frequency of PZT using the circuit output voltage in Figure 5.1.

In light of these results for investigating the resonance frequencies of the piezoelectric materials, a small difference was seen in comparison to the theoretically calculations. According to the calculations using Equation (2.1), by taking the speed of sound in PZT as 3970 m/s (Shung, 1996)), for a 500 μm thick, 0.5 mm × 0.5 mm PZT plate, thickness mode resonance frequency should be 3.97 MHz. The differences in the

resonance frequencies between the theoretical and experimental values may be caused by the epoxy sealing of the wire connection points on the material. Also, the material dimensions may not be exact since the piece was cut manually.

5.2 Testing the Feasibility of Modulation Effect

According to the Zhu and colleagues, if the load resistor is connected in series to two piezoelectric layers, the current, the voltage and the power dissipated depend on the value of the load resistance The value of the load resistance also significantly influences the vibrational characteristics of piezoelectric material, including the vibrational amplitude and the resonant frequency (Zhu, Worthington, & Njuguna, 2009). In addition, they stated that the maximum power output of piezoelectric material does not occur at the maximum vibrational displacement, nor does the maximum power output coincide with the optimum load resistance (Zhu et al., 2009). In this direction, first, the optimum potentiometer (500 Ω) was connected to the PZT to investigate the feasibility of modulation using a load resistor. Once the change in the amplitude of the echo signal was detected by varying the resistor then the optimum resistance value for the maximum modulation was calculated. This value was used as a design parameter in implementation of the electronic circuit that would function as a variable resistor that would use the neural signals as the input and shunt different amounts of current from the piezoelectric element as a function of neural signal amplitudes.

5.2.1 Results and Discussion

To visualize the observed change and the related frequency band for this change in the amplitude of the echo signal, the data was transferred to the computer from the

oscilloscope memory. Matlab was used to analyze the data and show the effect of load resistance.

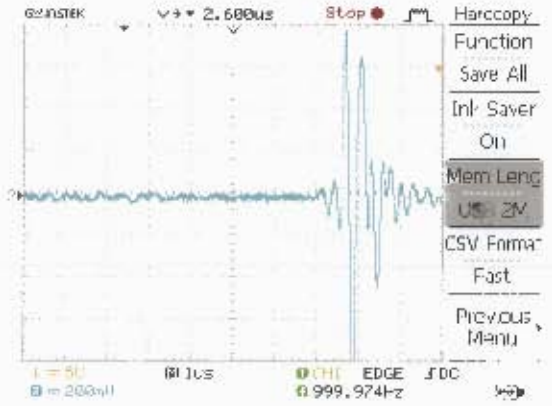

Figure 5.3 Maximum echo amplitude achieved by adjusting the potentiometer to 500Ω.

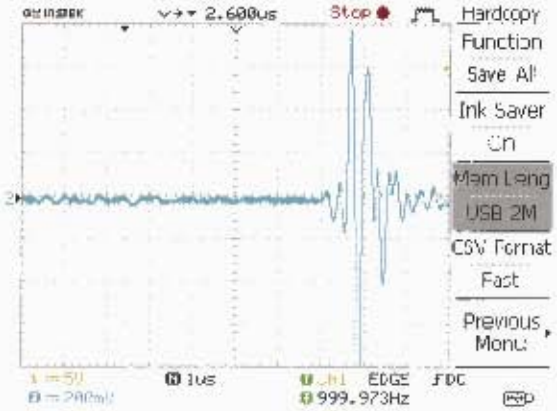

Figure 5.4 Minimum echo amplitude observed by adjusting the potentiometer to 1Ω.

According to the signals shown in Figure 5.3 and Figure 5.4, there is 40 mV_{pp} voltage difference between the cases of maximum and minimum loading of the PZT. After the signals are recorded, filtered and substracted from each other, it is observed that the maximum change in the echo signal occurs at the 4.22 MHz. Therefore, the maximum amplitude variation occurs around this frequency.

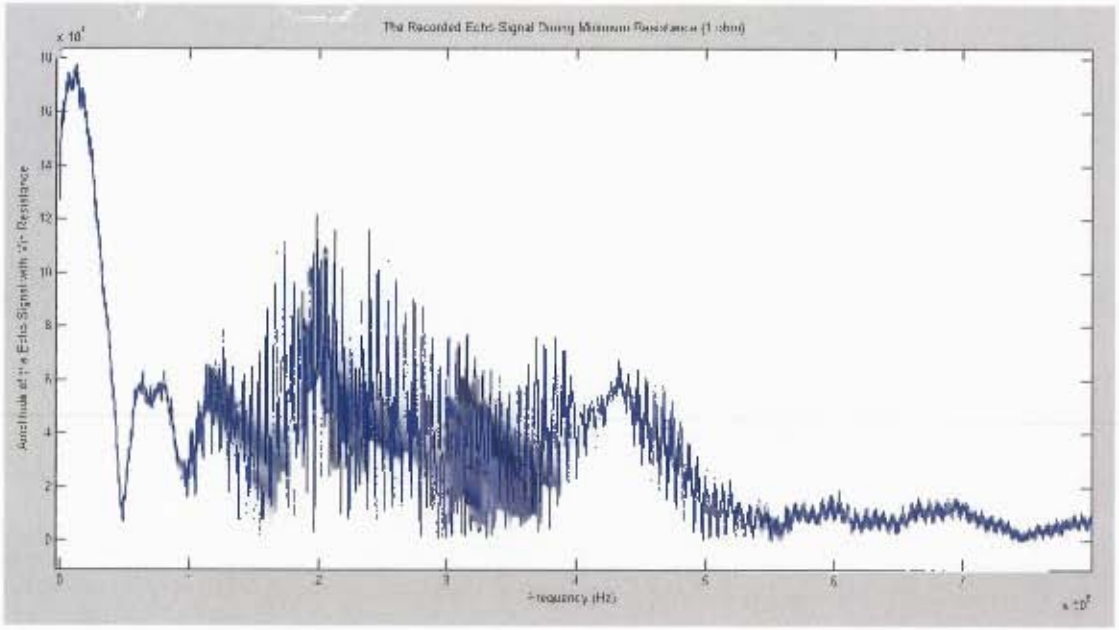

Figure 5.5 Power spectrum of the recorded echo signal that is reflected from the PZT while the potentiometer was set to minimum.

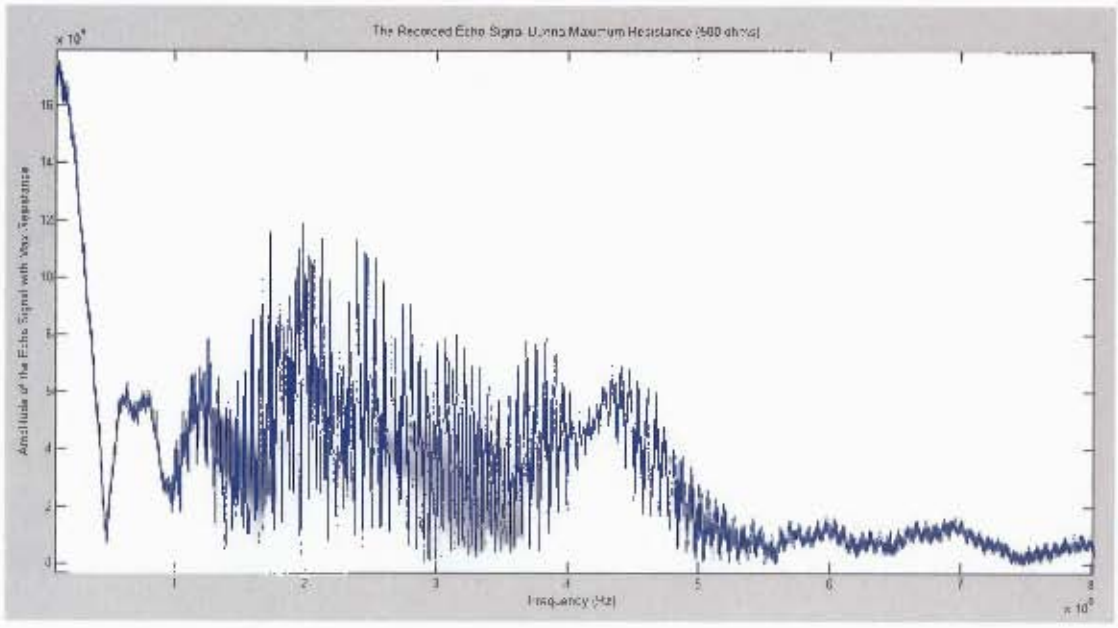

Figure 5.6 Power spectrum of the recorded echo signal that is reflected from the PZT while the potentiometer was set to maximum.

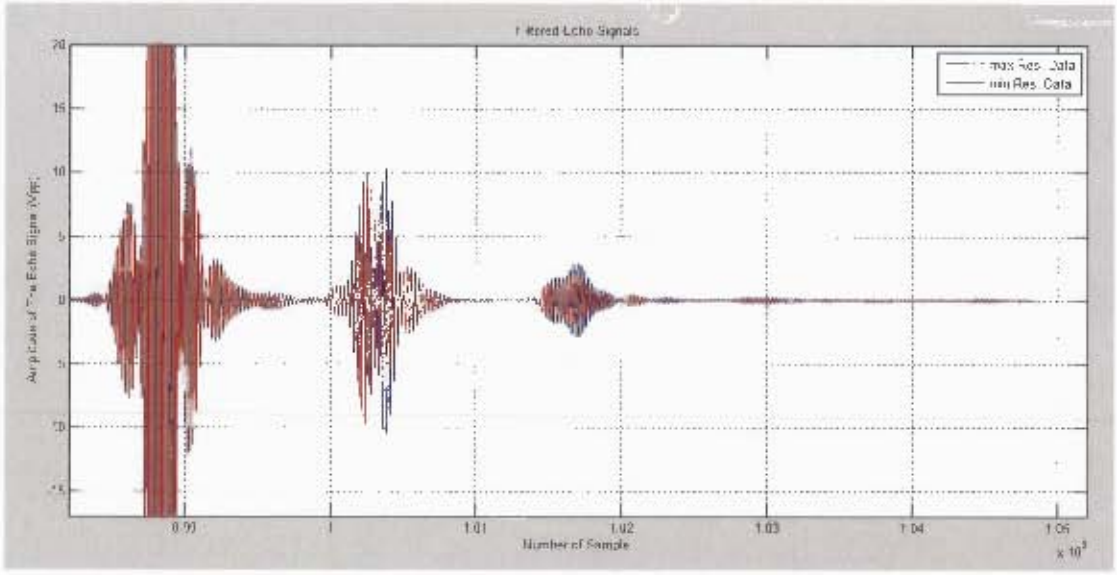

Figure 5.7 Filtered echo signals in the time domain.

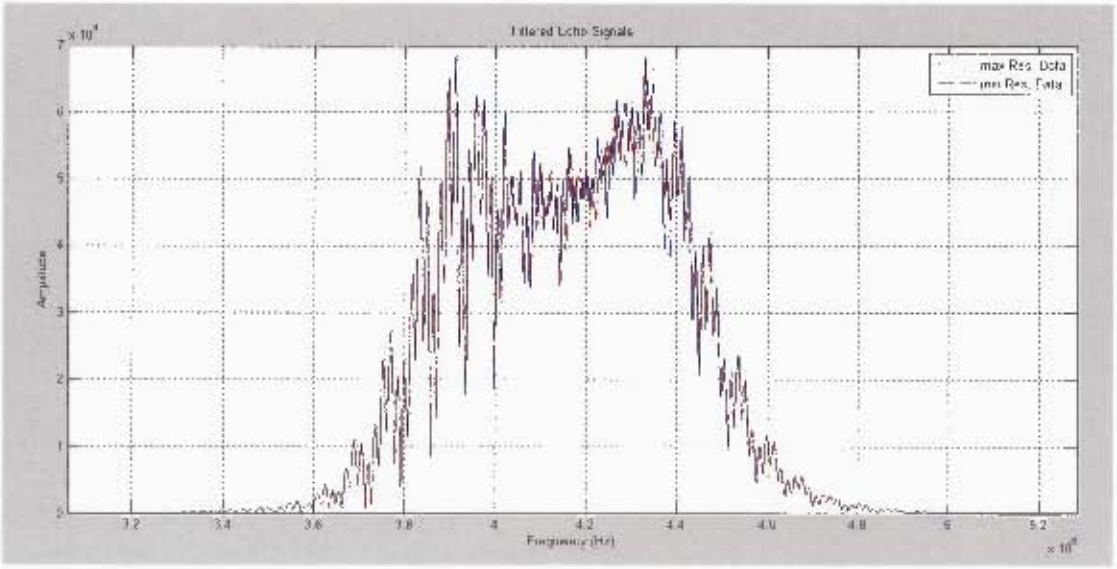

Figure 5.8 Power spectrum of the echo signals for maximum and minimum loading cases.

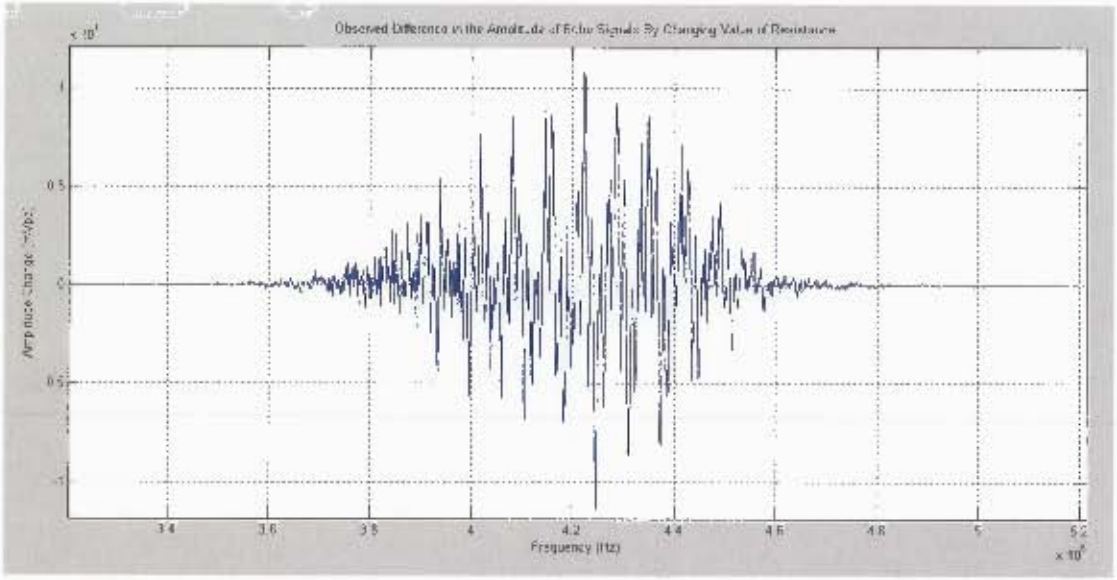

Figure 5.9 The differential power spectrum between maximum and minimum loads. The maximum difference is observed at 4.22 MHz.

5.3 Determination of the Optimum Load Resistance

While designing the circuit by the help of determining the optimum load resistance, the impedance value of the piezoelectric material at the relevant frequencies should also be estimated. With the given physical dimensions of the PZT (0.5 mm × 0.5 mm) used for this research, the optimum resistance value, when assumed that there is no effect of additional capacitive sources such as oscilloscope and probe, was obtained as 5 kΩ according to Equation (5.1) (Zhu et al., 2009).

$$Ropt = \frac{1}{\omega \times C} \tag{5.1}$$

In addition, it is also important to define the power range that the circuit can be driven to. For this reason, voltage measurements were made at specific load resistance values.

5.3.1 Results and Discussion

In terms of voltage measurements and dissipated power, two significant graphs with arbitrarily selected values of resistors (varying from 100 Ω to 1.5 MΩ) are plotted. Even though the resistors from 474 Ω to 1.2 kΩ seems to be the best choices to obtain the most efficient energy harvesting, a closer value to 2.37 kΩ was considered because of the trade-off between optimum load effect and required power for driving the MOSFETs in the designed circuitry.

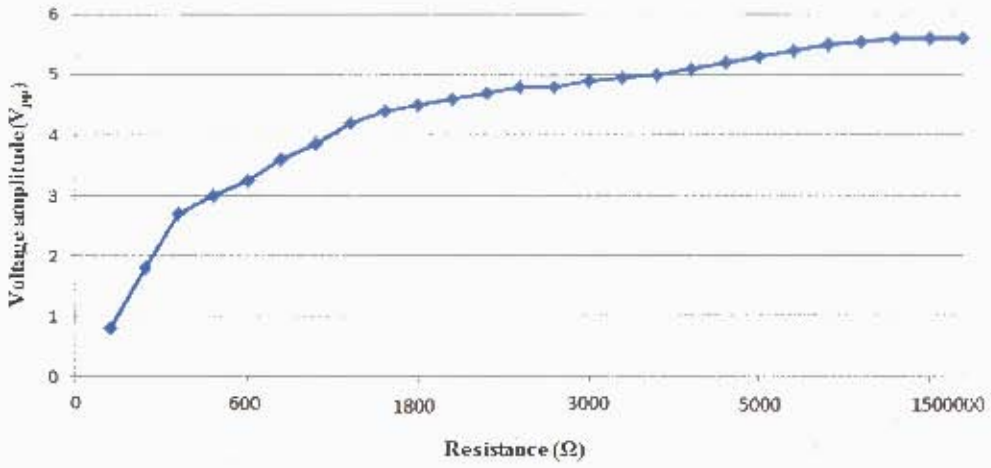

Figure 5.10 Voltage measurements from different load resistor values.

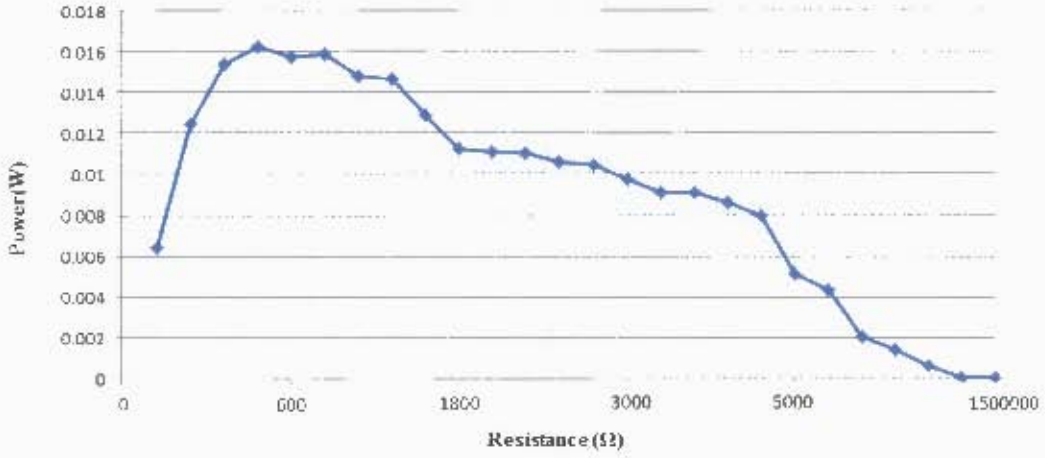

Figure 5.11 Dissipated power vs. the load resistor

5.4 Simulation and Implementation of the Design

LTspice (version 4.19u) is used to simulate the circuit before the implementation step. The design and its components are determined with reference to a previous Master's thesis carried out in the same laboratory (Hua & Sahin, 2013; Meng, 2012). In this simulation, the biological signal is defined as 100 μV_{pp}, 1 kHz sine wave and PZT is simulated as a current source and a resistance in parallel to the source. Also, in the model of PZT, frequency of the source voltage is determined from the frequency of the echo pulses. Thevénin equivalent of this source and parallel resistance is taken into account as a model of PZT and the value of the optimum load resistance that was obtained earlier.

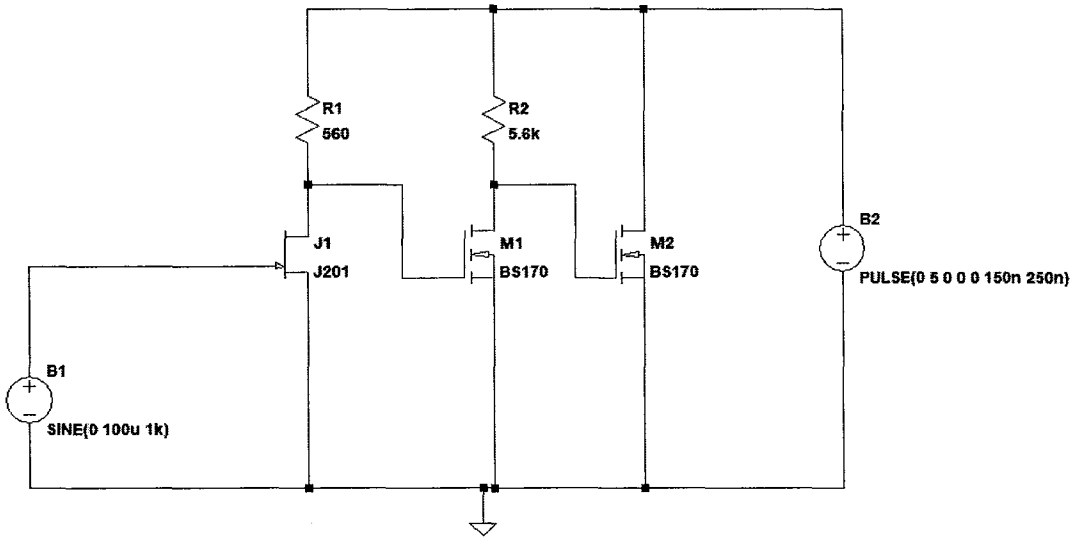

Figure 5.12 Circuit design for modulating the backscattered signal.

5.4.1 Simulation Results and Discussion

In the first stage of the circuit, the input, 100 μVpp 1 kHz sine wave signal is amplified by 37.48 dB. Then, this output appears as a 20 mVpp AC signal riding on a DC level of

1.022 V as shown in Figure 5.11. In this specific application, it was difficult to compensate the gain and reach optimum modulation index by trial and error method.

At 1 kHz and 4 MHz, most significant frequency components of the output signal of the circuit were observed by applying FFT shown in Figure 5.14 and Figure 5.15. It proves that the simulation accurately predicted the modulation effect. Besides, because of the capacitive effects the square wave at 4 MHz looks distorted as shown in Figure 5.16. This problem might be arisen from the parasitic capacitors in the MOSFETs.

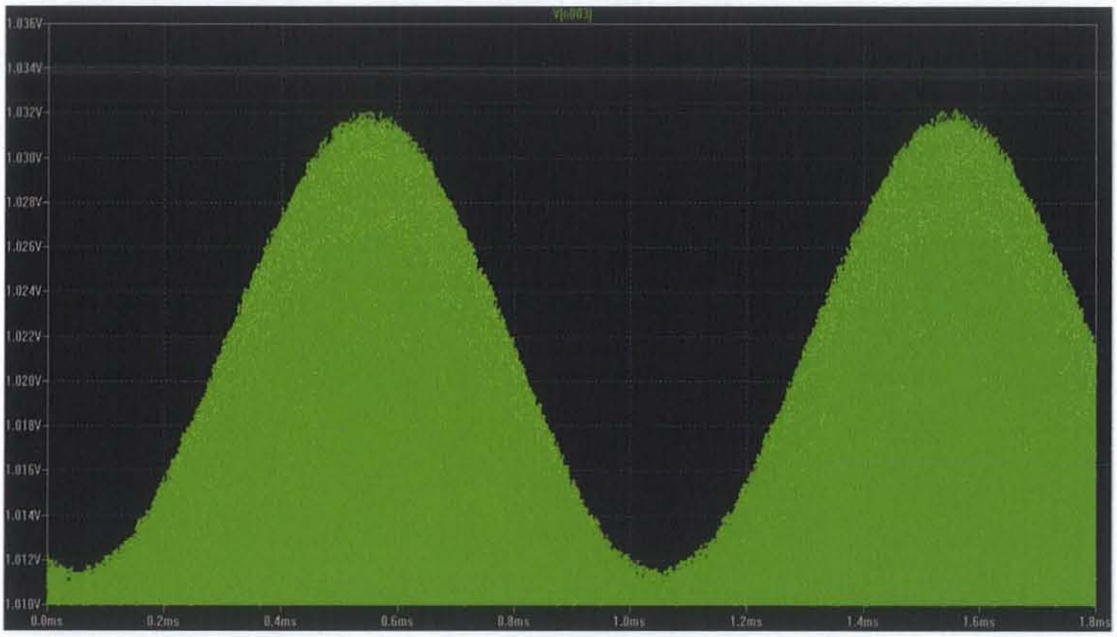

Figure 5.13 1 kHz modulated signal from the simulations.

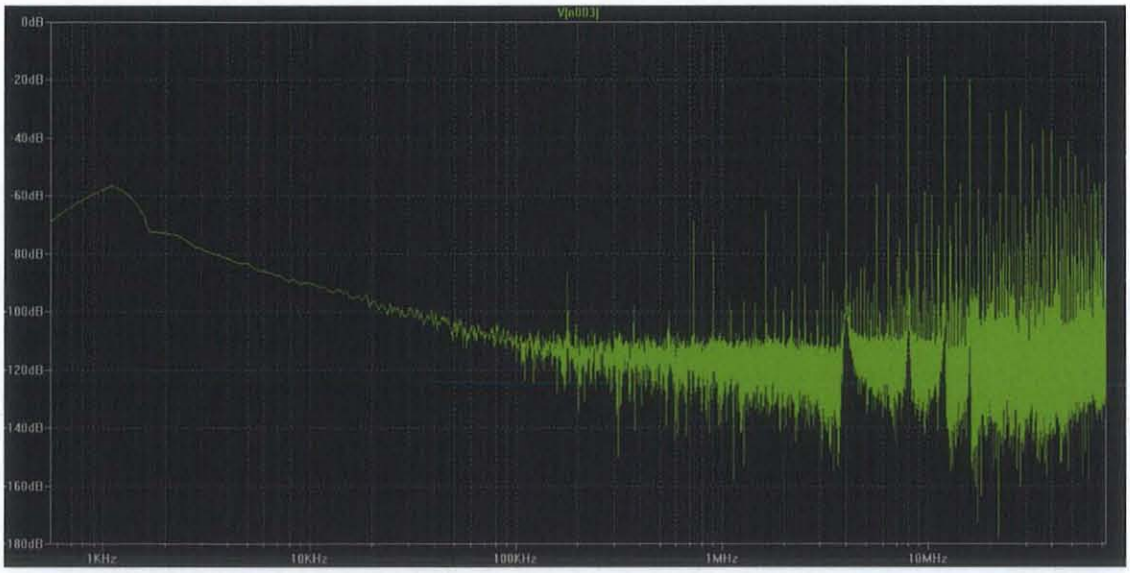

Figure 5.14 FFT of the simulated output signal.

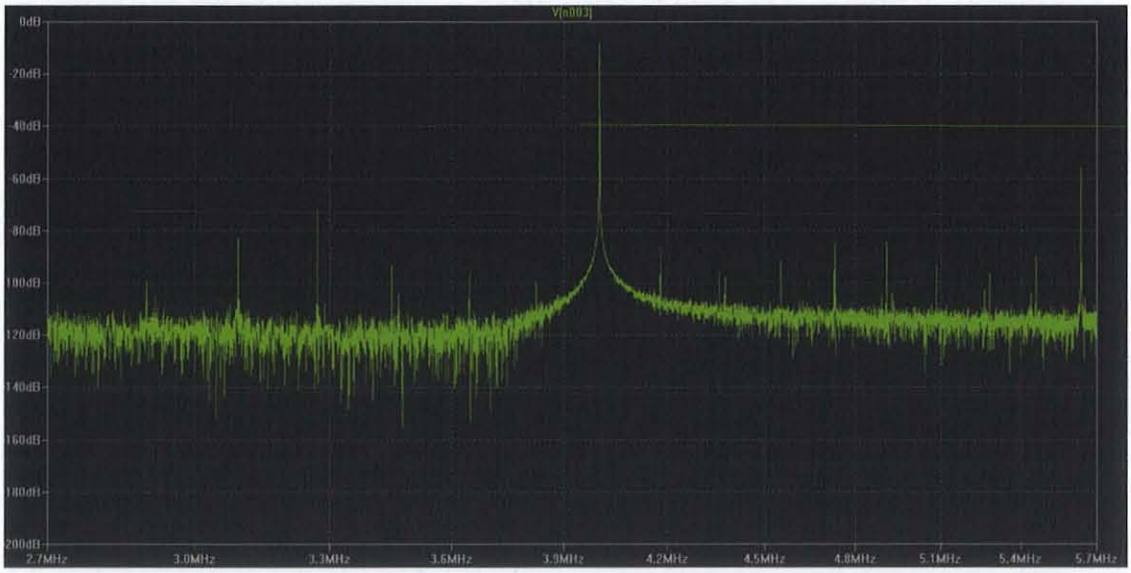

Figure 5.15 FFT of the simulated output signal as zoomed in at 4 MHz.

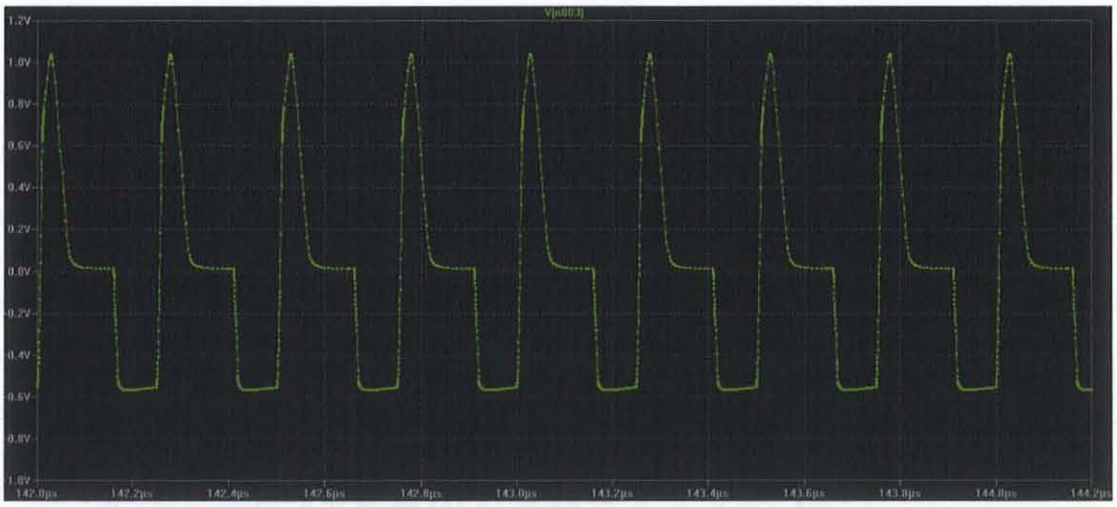

Figure 5.16 4 MHz square wave pulses at the output of the MOSFET that are modulated by the 1 kHz sine wave.

5.4.2 Implementation Results and Discussion

The circuit is built following the results of simulation and connected to the experimental set up.

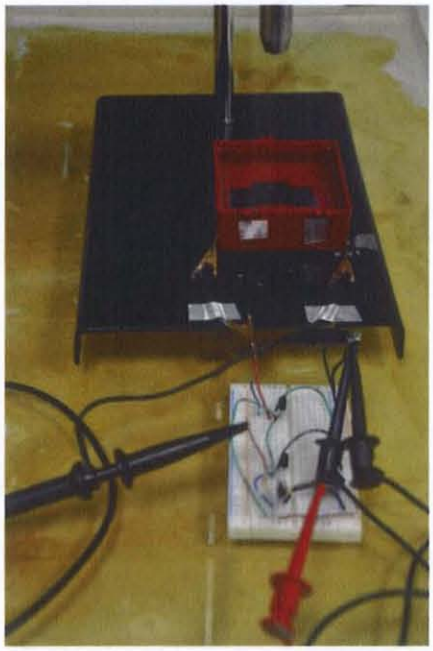

Figure 5.17 Constructed circuit on a breadboard and connected to the PZT.

Then, after driving the PZT without using any power supply, the backscattered signal is received by the transducer with the modulation of 12 mVpp of message wave.

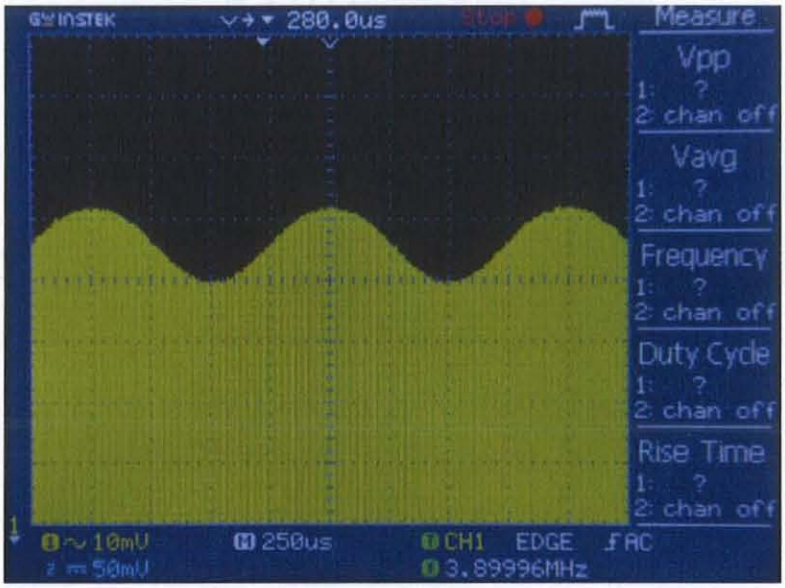

Figure 5.18 Modulated signal that has an amplitude (12mVpp) near the value predicted by simulation results.

CHAPTER 6

CONCLUSION AND FUTURE WORK

6.1 Conclusion

In most recent studies, there are major difficulties in achieving reliable implantable neural recording systems that can serve as brain-machine interfaces (BMI). Therefore, wired connections from implanted electrodes to the extracorporeal system are often preferred. To this end, this research was conducted to test the feasibility of an ultrasonic neural interface system that is based on modulation of the backscattered signal. We proposed that if the neural signal is sensed effectively by the internal unit and used to modulate the reflected signal off of a piezoelectric piece, the neural signal can be extracted by an external unit that receives this echo signal. To demonstrate the feasibility of this technique, the echo signal from a piezoelectric element was analyzed and the effect of the load resistor was demonstrated. Next, an electronic amplifier circuit was built to demonstrate that the modulation of the echo signal can be controlled as a function of the neural signal.

As the piezoelectric material, a PZT piece with 500 μm thickness was chosen. It was cut into the dimension of 0.5 mm × 0.5 mm. In order to achieve low impedance and high energy transfer through the medium, the coupling factor, dielectric constant, wave velocity of the piezoelectric materials were taken into account. Once the PZT was fabricated, it was tested to see if the desired resonance frequency could be obtained. Then, measurements of power and load resistance of the circuit design were made. To verify the experimental results, computer simulations were also conducted. All of these results were used for the implementation of the circuit design of such a wireless

implanted recording system. The amplifier with 37.48 dB gain was assembled and 12 mV_{pp} modulated signal was obtained without using any kind of power supply to drive the circuitry. Therefore, it should be emphasized that, the circuit does not need battery since it uses the power harvested from the incoming acoustic signal sent by the external unit.

6.2 Future Work

The PZT material finds widespread usage as a transducer material in medical and biological ultrasound applications. Better optimized PZTs can be fabricated and even copolymer designs can be tested to improve the results in this project. Also, as a complementary subsystem, external unit design should be optimized, which was out of the scope of this project. A system based integrated design including the transducer, pulser, and receiver combined together can be an effective way of miniaturizing this system.

REFERENCES

Arnau, A., Soares, D. (2004). Piezoelectric transducers and applications. *Springer*, New York, NY.

Brown, L.F. (2000). Design considerations for piezoelectric polymer ultrasound transducers. *IEEE Trans Ultrason Ferroelectr Freq Control, 47*(6), 1377-1396. doi: 10.1109/58.883527

Colucci, V., Strichartz, G., Jolesz, F., Vykhodtseva, N., Hynynen, K. (2009). Focused ultrasound effects on nerve action potential in vitro. *Ultrasound Med Biol, 35*(10), 1737-1747. doi: 10.1016/j.ultrasmedbio.2009.05.002

Devaraju, V (2013). Design, development and characterization of wideband polymer ultrasonic probes for medical ultrasound applications. Ph.D. Thesis, *Drexel University,* Philadelphia, PA.

Ferguson, J. E., & Redish, A. D. (2011). Wireless communication with implanted medical devices using the conductive properties of the body. *Expert Rev Med Devices, 8*(4), 427-433. doi: 10.1586/erd.11.16

Foster, F. S., Harasiewicz, K. A., & Sherar, M. D. (2000). A history of medical and biological imaging with polyvinylidene fluoride (PVDF) transducers. *IEEE Trans Ultrason Ferroelectr Freq Control, 47*(6), 1363-1371. doi: 10.1109/58.883525.

Gavrilov, L. R., Tsirulnikov, E. M., & Davies, I. A. (1996). Application of focused ultrasound for the stimulation of neural structures. *Ultrasound Med Biol, 22*(2), 179-192.

Gosselin, B. (2011). Recent advances in neural recording microsystems. *Sensors (Basel), 11*(5), 4572-4597. doi: 10.3390/s110504572

Harrison, R., Watkins, P. T., Kier, R. J. (Jan 2007). A low-power integrated circuit for a wireless 100-electrode neural recording system. *IEEE Journal of Solid-state Circuits, 42*, 123-133.

Hendee, W. R., and Ritenour, E. R. (2002). Medical imaging physics. *Wiley-Liss, Inc.,* New York, NY. *Fourth Edition*, 303-353.

Hoskins, P. R., Martin, K., and Thrush, A. (Jun 2010). Diagnostic ultrasound: Physics and equipment. *Cambridge University Press,* New York, NY.

Hua, M., Sahin, M. (2013). An electroacoustic recording device for wireless sensing of neural signals. *Conf Proc IEEE Eng Med Biol Soc*, 3086-3088. doi: 10.1109/EMBC.2013.6610193

Hua, M. (2012). A method for remote sensing of electrophysiological signals. M.S. Thesis, *New Jersey Institute of Technology University,* Newark, NJ.

Nagy, P. B. (2011). Ultrasonic nondestructive evaluation. *Class notes for nondestructive evaluation of ultrasound, School of Aerospace Systems, University of Cincinnati*, Cincinnati, OH.

Neihart, N., & Harrison, R. (2004). A low-power FM transmitter for use in neural recording applications. *Conf Proc IEEE Eng Med Biol Soc, 3*, 2117-2120. doi: 10.1109/IEMBS.2004.1403621

Neihart , N. M., & Harrison, R. R. (2005). Micropower circuits for bidirectional wireless telemetry in neural recording applications. *IEEE Trans Biomed Eng, 52*(11), 1950-1959. doi: 10.1109/TBME.2005.856247

Obeid, I., Nicolelis, M. A., & Wolf, P. D. (2004). A multichannel telemetry system for single unit neural recordings. *J Neurosci Methods, 133*(1-2), 33-38.

Roy, S., & Wang, X. (2012). Wireless multi-channel single unit recording in freely moving and vocalizing primates. *J Neurosci Methods, 203*(1), 28-40. doi: 10.1016/j.jneumeth.2011.09.004

Safari, A., Akdogan, E. K. . (2008). Piezoelectric and acoustic materials for transducer applications. *Springer*, New York, NY.

San Emeterio, J. L. (1997). Determination of electromechanical coupling factors of low Q piezoelectric resonators operating in stiffened modes. *IEEE Trans Ultrason Ferroelectr Freq Control, 44*(1), 108-113. doi: 10.1109/58.585203

Schwartz, R. W., Ballato, J., Haertling, G. H. (2003). Piezoelectric and electrooptic ceramics. *Marcel Dekker Inc.*, New York, NY.

Seo, D., Carmena, J. M., Rabaey, J. M., Alon, E., & Maharbiz, M. M. (2013). An ultrasonic, low power solution for chronic brain-machine interfaces. e-print arXiv: 1307.2196

Shung, K. K. (1996). Ultrasonic transducers and arrays. *IEEE, Engineering in Medicine and Biology Magazine, 15*(6). doi: 10.1109/51.544509

Vijaya, M. S. (2013). Piezoelectric materials and devices. *CRC Press:* Boca Raton, FL.

Zhang, D., Wang, D., Yuan, J., Zhao, Q., Wang, Z. , Cao, M. (2008). Structural and electrical properties of PZT/PVDF piezoelectric nanocomposites prepared by cold-press and hot-press routes. *Chin. Phys. Lett, 25*.

Olympus NDT (2006), Ultrasonic transducers technical notes, http://www.olympus-ims.com/data/File/panametrics/UT-technotes.en.pdf [accessed on 12/18/13].

Zhu, M., Worthington, E., Njuguna, J. (2009). Analyses of power output of piezoelectric energy-harvesting devices directly connected to a load resistor using a coupled piezoelectric-circuit finite element method. *IEEE Trans Ultrason Ferroelectr Freq Control, 56*(7), 1309-1318. doi: 10.1109/TUFFC.2009.1187